Virus Genes (2013) 47:439–447
DOI 10.1007/s11262-013-0970-7

Molecular characterization of human parainfluenza virus type 1 in infants attending Mbagathi District Hospital, Nairobi, Kenya: a retrospective study

Joshua K. Kiptinness · Eyako K. Wurapa · Fred Wamunyokoli · Wallace D. Bulimo

Received: 26 March 2013 / Accepted: 5 August 2013 / Published online: 17 August 2013

Abstract Human parainfluenza virus type 1 (HPIV-1), a paramyxovirus, is a leading cause of pediatric respiratory hospitalizations globally. Currently, there is no clinically successful vaccine against HPIV-1. Hence, there is a need to characterize circulating strains of this virus to establish the feasibility of developing a vaccine against the virus. The variable HPIV-1 hemagglutin–neuraminidase (HN) protein is found in the envelope of HPIV-1, where it initiates the infection process by binding to cellular receptors. HN is also the major antigen against which the human immune response is directed against. The present study focused on identifying mutations in the HN gene that would be useful in understanding the evolution of HPIV-1. 21 HPIV-1 isolates were obtained after screening nasopharyngeal samples from patients with influenza-like illness. The samples were collected from Mbagathi District Hospital Nairobi from the period July 2007 to December 2010. RT-PCR was carried out on the isolates using HN-specific primers to amplify a 360 nt in the most polymorphic region and the amplicons sequenced. Genomic data were analysed using a suite of bioinformatic software. Forty eight polymorphic sites with a total of 55 mutations were identified at the nucleotide level and 47 mutations at 23 positions at the amino acid level. There was more radical nonsynonymous amino acid changes (seven positions) observed than conservative nonsynonymous changes (one position) on the HN gene fragment. No positively selected sites were found in the HN protein. The result from the analysis of 21 HPIV-1 Mbagathi isolates demonstrated that the HN gene which is the major antigenic target was under purifying (negative) selection displaying evolutionary stasis.

Keywords HPIV-1 · HN gene · Kenya · Population genetics

Electronic supplementary material The online version of this article (doi:10.1007/s11262-013-0970-7) contains supplementary material, which is available to authorized users.

J. K. Kiptinness (✉)
Institute of Tropical Medicine and Infectious Diseases (ITROMID), Jomo Kenyatta University of Agriculture and Technology, Nairobi, Kenya
e-mail: kimuttai@gmail.com

E. K. Wurapa · W. D. Bulimo
Department of Emerging Infectious Diseases (DEID), The United States Army Medical Research Unit in Kenya (USAMRU-K), Nairobi, Kenya
e-mail: eyako.wurapa@usamru-k.org

W. D. Bulimo
e-mail: wallace.bulimo@usamru-k.org

F. Wamunyokoli
Department of Biochemistry, Jomo Kenyatta University of Agriculture and Technology, Nairobi, Kenya
e-mail: fwamunyokoli@gmail.com

W. D. Bulimo
Department of Biochemistry, School of Medicine, University of Nairobi, Nairobi, Kenya

Background

Human parainfluenza viruses (HPIVs) are enveloped, non-segmented, single-stranded, negative-sense RNA viruses belonging to the family *Paramyxoviridae*. HPIV-1 is a major cause of lower respiratory infections in infants, young children, the immunocompromised, the chronically ill, and the elderly [19]. HPIV-1 is responsible for approximately 6 % of pediatric respiratory tract disease [13]. It has worldwide

distribution and probably contributes significantly to childhood mortality in the developing world [9]. In Kenya, acute respiratory infection (ARI) accounts for 20 % of hospital admissions and more than half of these are children under 5 years of age [23]. In attempts to prevent infection with HPIV-1, different vaccine strategies have been employed. These include use of killed viruses [8], attenuated viruses [27], virus subunits [3], virus recombinants [10], and Jennerian vaccines [20]. Clinical trials initiated with the several different vaccine candidates have each demonstrated some promise [5, 27, 28], to date no vaccines have yet been successfully clinically proven. There is therefore need to characterize the circulating strains of this virus in order to establish the feasibility of developing a viable vaccine against the virus.

The variable HPIV-1 hemagglutin–neuraminidase (HN) protein responsible for initiating the infection process by binding to cellular receptors, is found on the surface of HPIV-1 virion. The present study focused on identifying mutations in the antigenically important HN gene that would be useful in understanding evolution of HPIV-1, hence feasibility of developing HN-targeting vaccines.

Results

Viral cell culture

Amongst the 25 HPIV-1 cultured isolates, 15 of them showed CPE after incubation for between 7 and 10 days.

Immunofluorescence assay

Of the 25 cultures screened for HPIV-1 by IFA, 21 tested positive as shown by the apple-green fluorescence among infected cells.

RT rt PCR

Fifteen isolates which showed CPE upon inoculation in LLCMK2 cells and were positive on IFA displayed low (C_T) values ranging from 22 to 28. The above results are summarised in Table 1.

RT PCR

A DNA fragment of 360 bp was obtained by PCR with the reference C35 strain. The 21 test cases of the HPIV-1 results were consistent with those obtained in RTrtPCR and generated the expected 360-bp band.

Table 1 Usage of real time RT-PCR, CPE, and IFA diagnostic assays for the detection of HPIV-1 in culture

Isolate name	C_T value	Presence of CPE?	IFA
MBG/07/06/01	27	YES	+
MBG/07/07/02	24	YES	+
MBG/07/08/03	26	YES	+
MBG/08/03/04	UNDET	NO	−
MBG/08/04/05	38	NO	+
MBG/08/04/06	40	NO	+
MBG/08/04/07	UNDET	NO	−
MBG/08/04/08	38	NO	+
MBG/08/04/09	26	YES	+
MBG/08/06/10	22	YES	+
MBG/08/09/11	37	NO	+
MBG/08/10/12	24	YES	+
MBG/08/10/13	25	YES	+
MBG/08/10/14	25	YES	+
MBG/08/10/15	25	YES	+
MBG/08/11/16	28	YES	+
MBG/09/09/17	24	YES	+
MBG/09/12/18	34	NO	+
MBG/10/01/19	28	YES	+
MBG/10/02/20	26	YES	+
MBG/10/03/21	40	NO	+
MBG/10/05/22	27	YES	+
MBG/10/05/23	27	YES	+
MBG/10/06/24	UNDET	NO	−
MBG/10/09/25	UNDET	NO	−
C35 (positive control)	20	YES	+
Negative control	UNDET	NO	−

The CT values represent the extent of positivity using the real-time RT-PCR assay. "UNDET" represents a absence of virus where us the numbers reflect inverse viral titres. Presence of virus using the CPE assay is shown by a "YES" and absence by "NO". Presence of virus in culture by IFA is denoted by "+" and absence of virus is denoted by "−"

Nucleotide sequence polymorphism

Forty-eight variable (polymorphic) sites with a total of 55 mutations were identified when the sequences were analyzed together. In addition, 11 synonymous changes were observed at positions 7305, 7356, 7362, 7422, 7437, 7479, 7740, 7506, 7509, 7512, and 7521 (using the Washington 1964 HPIV-1 reference strain numbering). Finally, 36 replacement changes (single nucleotide polymorphism) were observed at positions 7256, 7259, 7260, 7261, 7265,7265, 7279, 7291,7295, 7298, 7299, 7311, 7315, 7316, 7316, 7320, 7328, 7328, 7345, 7349, 7384, 7390, 7391, 7393, 7418, 7420, 7454, 7459, 7470, 7486, 7493, 7499, 7509, 7510, 7511, and 7513 (Fig. 1).

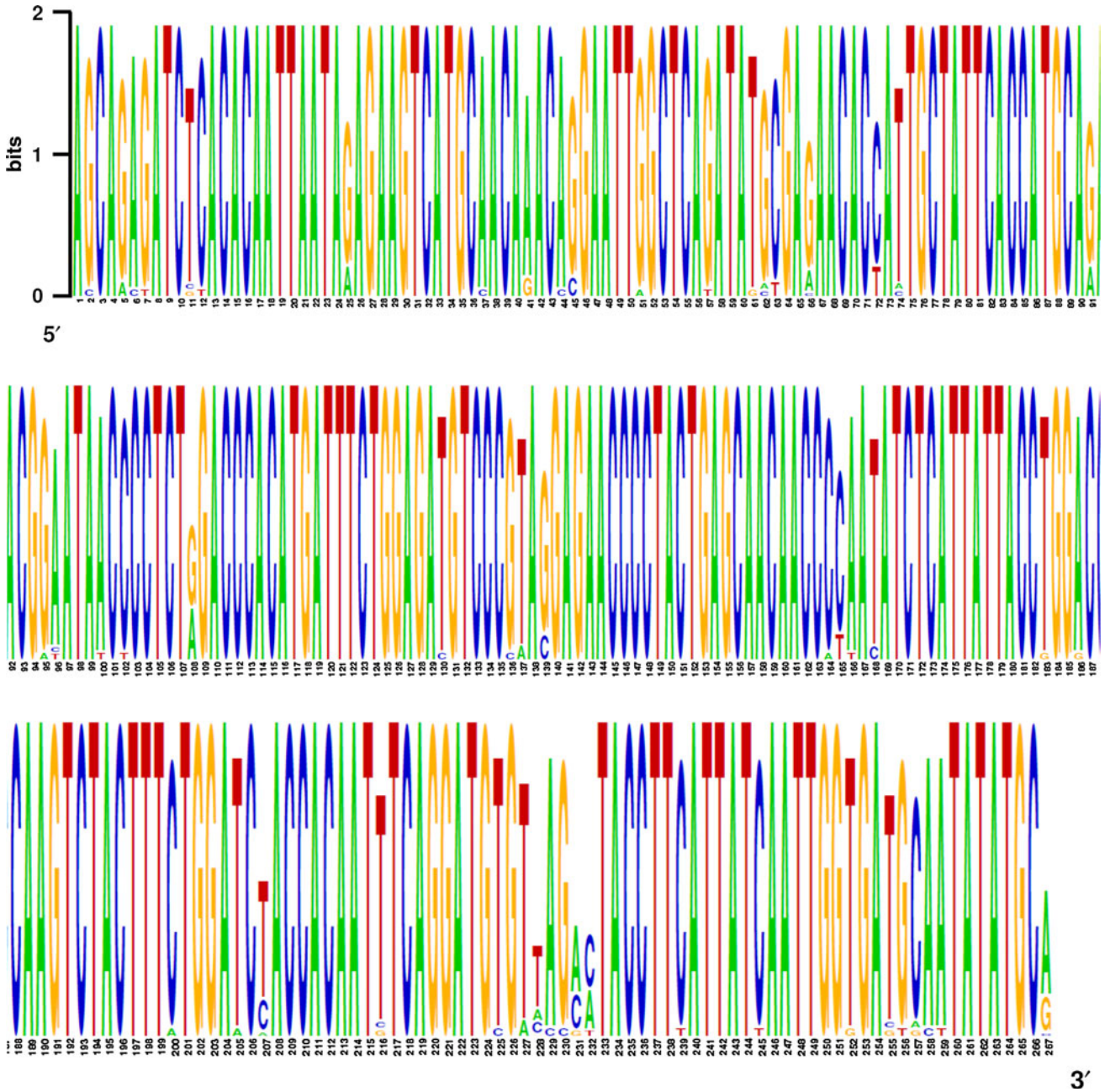

Fig. 1 Nucleotide alignment of HPIV1 HN region from 7254 to 7521 of 21 HPIV-1 Mbagathi isolates. A fragment of HN gene ranging from nucleotide 7254 to 7521 from 21 Mbagathi isolates, 6 reference strains, C35 positive control were aligned. Each logo consists of stacks of symbols, one stack for each position in the sequence. The overall height of the stack indicates the sequence conservation at that position, while the *height of symbols* within the stack indicates the relative frequency of each nucleic acid at that position. The polymorphisms visualization was done using seqlogo

Amino acid sequence substitutions amongst the Mbagathi virus isolates compared to reference strains

The portion (position 118–205) of the HN protein analyzed consisted of 89 amino acids (according to the Washington 1964 HPIV-1 reference strain numbering). This protein region corresponds to the DNA region whose nucleotide sequences had been determined. There were 47 mutations in 23 positions on the HN protein.

Codon-based test of neutrality for analysis between sequences

The probability of $dN < dS$ was <1 ($dN < dS < 1$). Values of $P < 0.05$ are considered significant at the 5 % level. The

variance of the difference was computed using the bootstrap method (500 replicates). Analyses were conducted using the Nei and Gojobori method [21]. Using Kumar's method [15], it was observed that $dS = 0.1230$ and $dN = 0.0890$; and hence, $\varphi = dN/dS = 0.0890/0.1230 = 0.7235$

Radical and conservative nonsynonymous substitutions

Radical synonymous substitutions were observed at seven codons at positions 127 (E–K), 131 (N–H), 120 (R–S), 137 (Q–H), 162 (C–R), 194 (R–S), and 195 (R–T) (Table 2). A single conservative nonsynonymous substitution was observed at codon 140 (E–D).

Tajima's test of HPIV-1 HN

The overall value of Tajima's D for the HN gene is negative (−1.87251); statistical significance, $P < 0.05$; Fu and Li's D* test statistic: −2.61989; statistical significance: * $P < 0.05$; Fu and Li's F* test statistic: −2.79312; statistical significance: * $P < 0.05$.

Transition/transversion ratio

Looking at the field isolates, the average nucleotide frequencies were: T (24.9 %), C (25 %), A (32.5 %), and G (17.6 %). It was observed that out of the 55 mutations, 25 (45 %) lead to A–G [11], C–T [15] transitions versus 30 (55 %) A–C [9], A–T [10], G–C [4], G–T [7] transversions. Using Kimura-2 parameters, the ratio of transition/transversion (ti/tv) was computed. Transversions were slightly more than the transitions.

Evolutionary tree HPIV-1 isolates

All the reference strains clustered together under one main branch with 67 % posterior probability, and further divided into two distinct branches. MBG 07/06/01 was on a separate branch from the rest of the isolates though all shared a common ancestor. In addition, MBG07/06/01 had 11 unique nucleotide substitutions that were specific to it only, while the rest of the isolates and reference strains had the same nucleotide at the respective positions. Most of the 2007–2008 isolates clustered together on a separate branch. Similar, the 2009–2010 isolates clustered together on another separate branch (Fig. 2). There were four distinct branches that were formed by corresponding amino acid sequences. As in the nucleotide clustering, the reference strains clustered on the same branch. However, M86786.1 clustered with C35 strain and MBG 07/07/02. MBG07/06/01 which was also on a separate branch in the nucleic acid tree clustered with MBG081014, MBG 080610, and MBG 070601 (Fig. 3).

Molecular evolution rate

The evolutionary rate was determined by use of an Evolutionary Calculator in DNAsp and was found to be 1.12×10^{-3} substitutions/site/year.

Table 2 Nonsynonymous radical substitutions at seven codon positions showed nonsynonymous radical substitutions

Codon position	Non-synonymous radical substitutions
127	E–K
131	N–H
120	R–S
137	Q–H
162	C–R
194	R–S
195	R–T

Discussion

This study confirmed Niesters' observations that the presence of HPIV-1 in a patient specimen (NP swab) can be detected by viral isolation in cultured LLC-MK2 with a time lag of 7–10 days and molecular (PCR) tests [22]. Viral load of a specimen is directly proportional to how quickly CPE develops in inoculated cultures of a susceptible cell line [31]. Whereas majority of patient specimens analyzed showed CPE's between days 7 and 10 and were later confirmed to have the virus using serology (IFA) and molecular (PCR) assays, some specimens that did not show any CPE upon inoculation in cell culture but indicated the presence of virus using the PCR assay.

The PCR assay detected virus in all the 25 isolates. However, using IFA, 21 of the 25 isolates were reported as containing HPIV-1. The failure of IFA to detect HPIV-1 virus in the 4 out of the 25 samples could be due to a low viral load or the presence of non-infectious virions in the specimen, which may have resulted from insufficient specimen or inappropriate transport or storage conditions (i.e., specimens were kept for extended period at room temperature or higher) consistent with the previous reports [7].

Another possibility is that the immunofluorescence assay to detect antigens has been associated with the sensitivity problems when the viral load is low [4].

Similar to the RT-PCR and IFA results, the 21 isolates stated above were also positive using the qRT-PCR assay. These observations validated the sensitivity and specificity of the IFA and RT-PCR assays, since qRT-PCR technique is the most sensitive technique for identifying the target

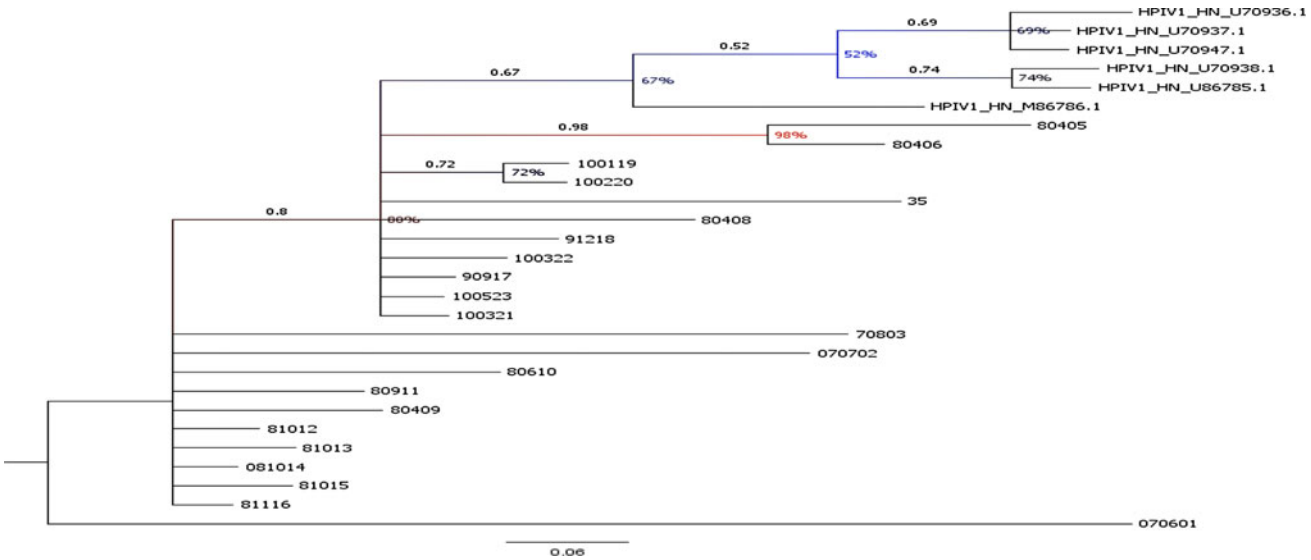

Fig. 2 Phylogenetic topology of MBG HPIV-1 HN gene using Mega 4. 0.06 nucleotide substitution/site. A topology tree prepared in MEGA4 and compared to type strains obtained from GenBank. The length of the *horizontal bar* is proportional to the number of nucleotide substitutions

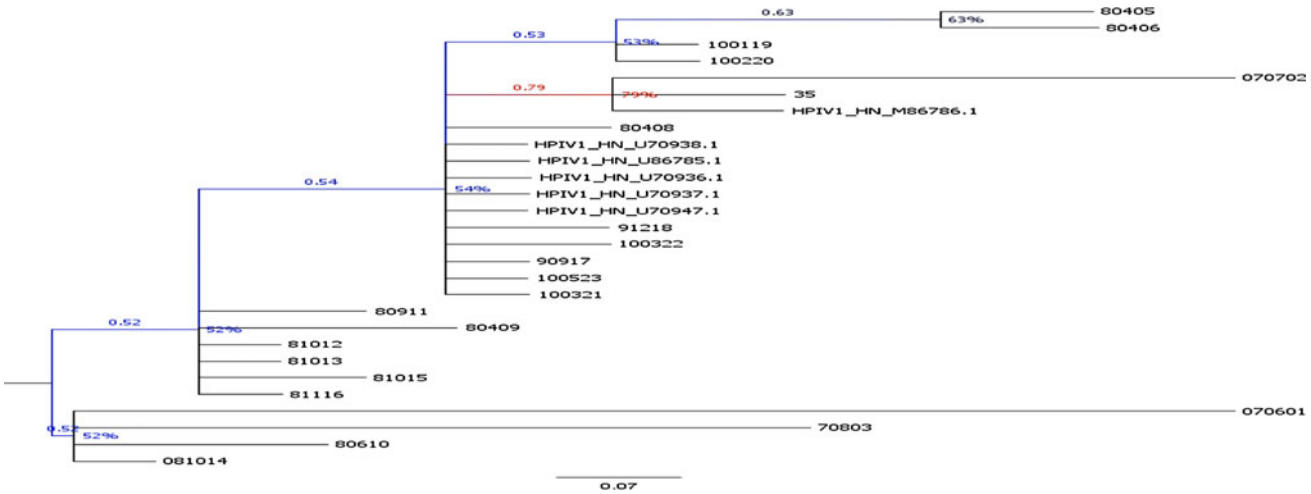

Fig. 3 Phylogenetic topology for MBG HPIV-1 HN amino acid sequences. 0.07aa substitution/site. Length of *horizontal bar* is proportional to the number of nucleotide substitutions

pathogens [30]. However, disparate isolates gave different C_T values. The lowest C_T value was 24 while the highest was 39. The high C_T values were indicative of low viral load of HPIV-1 in the sample isolates. This is supported by observations by Wan [32], who found a linear relationship between the copy number/viral particles present in the sample, and the C_T values on the chromatogram. C_T values have been used to estimate the viral load in a sample [1] with an inverse relationship, whereby high C_T values represent a low viral load, while a low C_T value show a high viral load.

When rt RT-PCR was performed on the nine samples that yielded virus when inoculated into culture, the mean C_T value was 25.6, whereas amongst the 12 that did not yield virus in culture, all had undetermined (ut) C_T value. These findings mirrored a similar study [2] that observed C_T values ranging from 27 to 42 amongst nasopharyngeal samples considered positive only by real-time PCR versus C_T values ranging from 18 to 22 for culture positive samples. The undetermined (ut) results may have been due to the degradation of viral RNA in the samples arising from multiple freeze–thaw cycles between the initial isolation of the HPIV and the RT-PCR procedures [6].

The present HPIV-1 isolates showed an overall high level of nucleotide sequence identity (94–98 %) of this HN amplified region. This result suggests that several lineages of highly conserved HN HPIV-1 were prevalent in the Mbagathi isolates. This is in line with the study findings of

Mizuta et al. [17], who found that the HN gene is highly conserved in HPIV-1. In the current study, the evident low polymorphism in HN gene can be attributed to both the factors, i.e., the short length (267 bp) of the region of the gene analyze and small sample size of 25.

A ti/tv of 0.8 means that there was a bias toward transition substitutions in this region of HN gene. Transition versus transversion bias has been shown to result from the relatively high rate of mutation of methylated cytosines to thymine [14]. In general, it is assumed that there is a universal bias in favor of transitions over transversions due to the underlying chemistry of mutation. Saturation of transitions at high levels of genetic divergence is commonly believed to explain the bias toward transition [18].

In this study, several tests of neutrality were applied to ascertain each other. Analysis of selection pressure in the isolates showed that *dS* substitutions predominated over *dN* substitutions, and no positively selected sites (substitution) were found in HN protein. This implied that the amino acid change was deleterious, purifying selection thus reducing its fixation rate, therefore $\varphi < 1$ [33]. Similar results were obtained by Mizuta et al. [17], who carried out a selection pressure analysis of HN gene HPIV-1 in Japan, and obtained a low *dN*/*dS* ratio of 0.17. It is also possible that this could result in stabilizing selection through the purging of deleterious variations that arise [11].

It was evident that all the 21 samples shared a common ancestor since they all were monophyletic. The nucleotide sequence tree suggests that the immediate ancestor for each of the two main branches further evolved into the variants within each main branch. The ladder-like phylogeny demonstrated by these trees suggests that the evolution of HPIV-1 is occurring with HN maintaining its function, and may be useful in predicting the emergence of antigenic variants of HPIV-1 circulating in the region.

The rate of molecular evolution (11.2×10^{-4} substitutions/site/year) was comparable to that obtained in another HPIV-1 genome study carried out in Japan [17] that found the rate to be 7.68×10^{-4} substitutions/site/year. MBG 07/06/01 seemed to evolve at a different rate than the rest of the isolates demonstrated by the distinct branching pattern and the unique substitutions shown in both the nucleotide and amino acid phylogenetic trees. It is possible that the genome properties other than size, such as polarity or structure, may be associated with substitutions of the viral genome [25].

Conclusions

The result from the analysis of 21 HPIV-1 Mbagathi isolates isolated in 2007–2010 demonstrated that their HN gene which is the major antigenic target was under purifying (negative) selection displaying evolutionary stasis. Overall, these results suggest that the HPIV-1 is antigenically and genetically stable, and therefore, amenable to easy vaccine targeting.

Methods

Study design and population

This study was a retrospective study carried out at the KEMRI-National Influenza Center. The study utilized 25 positive screened HPIV-1 isolates collected from infants aged 6–36 months attending Mbagathi District Hospital Nairobi from the period July 2007 to December 2010, which had been previously detected by cell culture and direct immunofluorescence. A prototype strain of HPIV-1 (strain C35) was obtained from the Centers for Disease Control and Prevention collection, Atlanta, GA, USA.

HPIV-1 isolation

Human parainfluenza virus type 1 viruses were amplified and isolated by inoculating patient samples in passage LLC-MK_2 cells (T75 flasks containing approximately 1.1×10^6 cells/ml and 1.1×10^7/flask). LLC-MK2 (ATCC CCL7.1) cells were grown in T75 flasks (Corning, NY, USA) with DMEM (Sigma-Aldrich Co Ltd, UK), supplemented with 10 % heat inactivated fetal bovine serum [12] in a CO_2 incubator—Thermoscientific model BBD 62220 (Thermoscientific Inc., CA, USA) at 37 °C, 5 % CO_2, 95 % humidity for 72 h. At 80 % ($\sim 8.8 \times 10^7$ cells/ml and 8.8×10^8 cells/flask) confluence, the cells were washed with Hanks balanced salt solution (Invitrogen, GIBCO) supplemented with 0.25 µg trypsin per ml and inoculated with 100 µl of homogenized isolate after pouring off the growth medium. The adsorption of the virus onto the LLC-MK2 cell cultures was enhanced by incubating at 37 °C for 1 h in a 5 % CO_2 incubator; then 1 ml of maintenance media was added (appendix IV). The cultures were then incubated in a 5 % CO_2 incubator and humidity of 80 % and observed for cytopathic effects after 48 h and up to 10 days and stored at −80 °C in a HERA Freeze ultra-low freezer (Thermoscientific, CA, USA). For the positive control, the prototype strain of HPIV-1 (strain C35) obtained from the Centers for Disease Control and Prevention collections, Atlanta, GA, USA was used. For the negative control, 1 ml of maintenance media was added to the cells.

HPIV-1 identification by immunofluorescence

Human parainfluenza virus type 1 in the supernatant was identified by the direct immunofluorescent antibody assay (IFA) using the SimulFluor™ Flu Para-1 MAb reagent

(Chemicon International, CA, USA). Positive and negative control slides were stained and included in each run for comparison.

RNA extraction

The QIAamp Viral RNA Mini spin protocol (Qiagen, Hilden, Germany) was used for RNA extraction. All isolates were extracted according to the manufacturer's instructions. In the negative control, sterile distilled water was added instead of specimen. For the positive control, the prototype strain of HPIV-1 (strain C35) obtained from the Centers for Disease Control and Prevention collections, Atlanta, Georgia was used.

Primer and probe design

The conventional PCR primers used in this study were designed using web-primer primer design (http://www.yeastgenome.org/cgi-bin/web-primer) from HPIV-1 HN strain Washington 1964 (Accession number AF457102, region: 6847–8740) and was selected to ensure that the size of the amplicon could be easily differentiated by agarose gel electrophoresis. The primers were ordered from Bioserve, MD, USA.

Primers and probes [29] used for RTrtPCR detection were ordered from ABI (Applied Biosystems Inc., CA, USA). Reverse transcription was performed using the 7500 fast Real Time RT PCR platform (Applied Biosystems Inc., CA, USA). Briefly, real-time reverse transcriptase PCR was performed in 25 µl of reaction mixture consisting of 12.5 µl of 2× one-step reverse transcription (RT)-PCR buffer (Ambion, CA, USA), one-step RT-PCR kit (containing dNTPs and MgCl), 0.25 µl of 5 pm/µl probe, 0.25 µl of 10 pm/µl forward and 10 pm/µl reverse primers, 5 µl of 23 ng/µl RNA template, 0.625 µl of enzyme, 6.125 µl of nuclease free water and the volume to 25 µl using double distilled water. The PCR thermal profile consisted of an initial cDNA step of 30 min at 50 °C followed by 15 min at 95 °C and 50 cycles of 30 s at 95 °C, 30 s at 55 °C, and 30 s at 72 °C. In the negative control, sterile distilled water was added instead of specimen. For the positive control, the prototype strain of HPIV-1 (strain C35) was used. RTrtPCR provided information on the viral load in each of the isolates, whereby low Ct values correlated with high viral loads. Primary amplification, detection, and data analysis were performed with Applied Biosystems Fast PCR 7500 platform (Applied Biosystems Inc., CA, USA).

HPIV-1 conventional PCR primers, reverse transcription, and primary amplification

All supernatants, found to be positive for HPIV-1 by RTrtPCR, were further tested by conventional RT-PCR to confirm the results. The primers used targeted a different region of the same gene as the real-time PCR. This was performed in 25 µl of reaction mixture consisting of 12.5 µl of 2× one-step reaction mixture containing DNTPs, $MgCl_2$, and reverse transcriptase (Invitrogen one-step RT-PCR kit), 1 µl Super script III Taq polymerase, 0.5 µl of the forward (20 pm/µl) and reverse (20 pm/µl) primers, 3 µl of 30 ng/µl RNA template, 7.5 µl of nuclease free water. The PCR thermal-cycling profile consisted of an initial cDNA synthesis step of 30 min at 50 °C, followed by denaturation for 2 min at 94 °C and 45 cycles (consisting of denaturation for 45 s at 94 °C, primer annealing for 45 s at 57 °C, and strand extension for 2 min at 68 °C). In the negative control, sterile distilled water was added instead of template RNA. For the positive control, RNA from the prototype strain of HPIV-1 (strain C35) was used. The expected product of 360 bp was detected by agarose gel electrophoresis on 2 % agarose.

Analysis of PCR products

Real time PCR products were analyzed using Applied Biosystems 7500 fast software. Conventional PCR products were analyzed by agarose gel electrophoresis on 2 % (w/v) agarose using 1XTBE (Promega, USA) as previously described [26].

Sequencing

Direct sequencing of the PCR product was carried out using the primers HPIV-1HNf and HPIV-1HNr on a 3500×1 genetic analyzer which uses a fluorescent-based DNA analysis system.

Data analysis

Sequences from both strands of the PCR product were viewed and edited using Bioedit sotware version 7.0.0. The edited sequences were saved as FASTA format. For each individual sequence, a nucleotide–nucleotide BLAST (BLASTN) search was done (http:/www.ncbi.nlm.nih.gov/BLAST/Blast.cgi) to confirm its identity.

The saved sequences were then imported into Muscle 3.6, and multiple sequence alignment was done against the reference Washington 1964 sequence (accession number M86786.1). The aligned sequences were visualized using Gene Doc version 5, and further confirmed using Clustal Omega nucleotide alignment function. The aligned nucleotide sequences (7254–7521) were used in the subsequent analysis. Polymorphic sites, neutrality test, and linkage disequilibrium and recombination, was determined using DnaSP version 5.10 as previously described [24], available at http:/www.ub.es.dnasp. Differences between synonymous

and nonsynonymous substitutions were tested with the method of Nei and Gjobori [21] available in the program; PAL2NAL version 14 as previously described [16], and phylogenetic trees were constructed using Mr. Bayes version 3.2 software and visualization by Fig tree version 1.3.1. The trees were further confirmed using Mega 4 and ClustalW.

Acknowledgments This work was supported by on the Global Emerging Infectious surveillance (GEIS) which is part of the American Armed Forces Health Surveillance Centre (AFHSC).

Conflict of interest The authors declare that they have no competing interests.

References

1. C. van de Alma Pol, M. van Anton Loon, F.W. Tom, J.G. Nicolaas, N. Monique, K.B. Els, S. Rob, W.A. John, W.A. John, Increased detection of respiratory syncytial virus, influenza viruses, parainfluenza viruses, and adenoviruses with real-time PCR in samples from patients with respiratory symptoms. J. Clin. Microbiol. **45**, 2260–2262 (2007)
2. R.G. Bredius, K.E. Templeton, S.A. Scheltinga, E.C. Claas, A.C. Kroes, J.M. Vossen, Prospective study of respiratory viral infections in pediatric hemopoietic stem cell transplantation patients. Pediatr. Infect. Dis. J. **23**, 518–522 (2004)
3. R.J. Brideau, N.L. Oien, D.J. Lehman, F.L. Homa, M.W. Wathen, Protection of cotton rats against human parainfluenza virus type 3 by vaccination with a chimeric FHN subunit glycoprotein. J. Gen. Virol. **74**, 471–477 (1993)
4. A.E. Casiano-Colon, B.B. Hulbert, T.K. Mayer, E.E. Walsh, A.R. Falsey, Lack of sensitivity of rapid antigen tests for the diagnosis of respiratory syncytial virus infection in adults. J. Clin. Virol. **28**, 169–174 (2003)
5. P. Durbin Anna, A.R.A. Karron, Progress in the development of respiratory syncytial virus and parainfluenza virus vaccines. Clin. Infect. Dis. **37**, 1668–1677 (2003)
6. J.E. Ecchevaria, D.D. Erdman, E.M. Swierkosz, B.P. Holloway, L.J. Anderson, Simultaneous detection and identification of human parainfluenza viruses 1, 2, and 3 from clinical samples by multiplex PCR. J. Clin. Microbiol. **36**, 1388–1391 (1998)
7. G. Eugene-Ruellan, F. Freymuth, C. Bahloul, H. Badrane, A. Vabret, N. Tordo, Detection of respiratory syncytial virus A and B and parainfluenza virus 3 sequences in respiratory tracts of infants by a single PCR with primers targeted to the L-polymerase gene and differential hybridization. J. Clin. Microbiol. **36**, 796–801 (1998)
8. C.A. Heilman, From the National Institute of Allergy and Infectious Diseases and the World Health Organization. Respiratory syncytial and parainfluenza viruses. J. Infect. Dis. **161**, 402–406 (1990)
9. K.J. Henrickson, S.M. Kuhn, L.L. Savatski, Epidemiology and cost of human parainfluenza virus types one and two infections in young children. Clin. Infect. Dis. **18**, 770–779 (1994)
10. X.L. Hu, R. Ray, R.W. Compans, Functional interactions between the fusion protein and hemagglutinin-neuraminidase of human parainfluenza viruses. J. Virol. **66**, 1528–1534 (1992)
11. R.R. Hudson, N.L. Kaplan, Deleterious background selection with recombination. Genetics **141**(4), 1605–1617 (1995)
12. R.N. Hull, W.R. Cherry, O.J. Tritch, Growth characteristics of monkey kidney cell strains LLC-MK1, LLC-MK2, and LLC-MK2(NCTC-3196) and their utility in virus research. J. Exp. Med. **115**, 903–918 (1962)
13. R.A. Karron, P.L. Collins, Parainfluenza viruses, in *Fields Virology*, 5th edn., ed. by D.M. Knipe, P.M. Howley, 2007, pp. 1497–1526
14. I. Keller, D. Bensasson, R.A. Nichols, Transition-transversion bias is not universal: a counter example from grasshopper pseudogenes. PLoS Genet. **3**(2), e22 (2007)
15. S. Kumar, K. Tamura, M. Nei, MEGA3: integrated software for molecular evolutionary genetics analysis and sequence alignment. Brief Bioinform **5**(2), 150–163 (2004)
16. S. Mikita, T. David, B. Peer, PAL2NAL: robust conversion of protein sequence alignments into the corresponding codon alignments. Nucleic Acids Res. **34**, 609–612 (2006)
17. K. Mizuta, M. Saitoh, M. Kobayashi, H. Tsukagoshi, Y. Aoki, T. Ikeda, C. Abiko, N. Katsushima, T. Itagaki, M. Noda, K. Kozawa, T. Ahiko, H. Kimura, Detailed genetic analysis of hemagglutinin-neuraminidase glycoprotein gene in human parainfluenza virus type 1 isolates from patients with acute respiratory infection between 2002 and 2009 in Yamagata prefecture, Japan. Virol. J. **8**, 533 (2011)
18. C. Moritz, T.E. Dowling, W.M. Brown, Evolution of animal mitochondrial DNA: relevance for population biology and systematics. Annu. Rev. Ecol. Syst. **18**, 269 (1987)
19. A.W. Mounts, H. Kaur, U.D. Parashar, T.G. Ksiazek, D. Cannon, J.T. Arokiasamy, L.J. Anderson, M.S. lye, Nipah Virus Nosocomial Study Group, A cohort study of health care workers to assess nosocomial transmissibility of Nipah virus, Malaysia, 1999. J. Infect. Dis. **183**, 810–813 (2001)
20. B.R. Murphy, Current approaches to the development of vaccines effective against parainfluenza viruses [review]. Bull. World Health Organ. **66**, 391–397 (1988)
21. M. Nei, T. Gojobori, Simple methods for estimating the numbers of synonymous and nonsynonymous nucleotide substitutions. Mol. Biol. Evol. **3**(5), 418–426 (1986)
22. H.G.M. Niesters, Clinical virology in real time. J. Clin. Virol. **25**, 3–12 (2002)
23. W.O. Ochieng, D.T.G. Hazlett, T.M. Bell, P.M. Tukei, G.R. Ademba, J.M. Magana, G.W. Gathara, E.M. Wafula, A. Pamba, J.O. Ndinya- Achola, T.K. Arap Siongoki, Viral etiology and epidemiology of acute respiratory infections in children in Nairobi, Kenya. Am J. Trop. Med. Hyg. **39**, 632–640 (1988)
24. J. Rozas, J.C. Sanchez-DelBarrio, X. Messeguer, R. Rozas, DnaSP, DNA polymorphism analyses by the coalescent and other methods. Bioinformatics **19**(18), 2496–2497 (2003)
25. R. Sanjuán, M.R. Nebot, N. Chirico, L.M. Mansky, R. Belshaw, Viral mutation rates. J. Virol. **84**(19), 9733–9748 (2010)
26. J. Sambrook, E.F. Frisch, T. Maniatis, *Molecular cloning: a laboratory manual*, 2nd edn. (Oxford University Press, London, 1989)
27. M.H. Skiadopoulos, J.M. Tatem, S.R. Surman, Y. Mitcho, S.L. Wu, W.R. Elkins, The recombinant chimeric human parainfluenza virus type 1 vaccine candidate, rHPIV3-1cp45, is attenuated, immunogenic, and protective in African green monkeys. Vaccine. **20**, 1846–1852 (2002)
28. R.S. Tang, R.R. Spaete, M.W. Thompson, M. MacPhail, J.M. Guzzetta, P.C. Ryan, Development of a PIV-vectored RSV vaccine: preclinical evaluation of safety, toxicity, and enhanced disease and initial clinical testing in healthy adults. Vaccine. **26**, 6373–6382 (2008)
29. K.E. Templeton, S.A. Scheltinga, M.R.C. Beersma, A.C.M. Kroes, E.C.J. Claas, Rapid and sensitive method using multiplex real-time PCR for diagnosis of infections by influenza A and

influenza B viruses, respiratory syncytial virus, and parainfluenza viruses 1, 2, 3, and 4. J. Clin. Microbiol. **42**, 1564–1569 (2004)
30. M.E. Terlizzi, B. Massimiliano, F. Sidoti, F. Sinesi, V. Rosangela, G. Stefano, C. Costa, C. Rossana, Quantitative RT real time PCR and indirect immunofluorescence for the detection of human parainfluenza virus 1, 2, 3. J. Virol. Methods **160**, 172–177 (2009)
31. D. Tian, W. Zhang, J. He, Y. Liu, Z. Song, Novel, real-time cell analysis for measuring viral cytopathogenesis and the efficacy of neutralizing antibodies to the 2009 influenza A (H1N1) Virus. PLoS One **7**(2), e31965 (2012)
32. C. Wan, Y. Huang, L. Cheng, G. Fu, S.H. Shi, H. Chen, C. Deng, F. Lin, J. Lin, The development of a rapid SYBR green I-based quantitative PCR for detection of duck circovirus. Virol. J. **8**, 465 (2011)
33. Z. Yang, J.P. Bielawski, Statistical methods for detecting molecular adaptation. Trends Ecol. Evol. **15**(12), 496–503 (2000)